

Magnetically Biased Inductors in Switching Converters

Master of Science thesis in Electric Power Engineering

Praveen Raju Hasbavi

Tejas Bharadwaj Prakash

DEPARTMENT OF ELECTRICAL ENGINEERING – DIVISION OF ELECTRIC POWER ENGINEERING

CHALMERS UNIVERSITY OF TECHNOLOGY
Gothenburg, Sweden 2021
www.chalmers.se

MASTER'S THESIS 2021

Magnetically Biased Inductors in Switching Converters

Praveen Raju Hasbavi
Tejas Bharadwaj Prakash



CHALMERS
UNIVERSITY OF TECHNOLOGY

Department of Energy and Environment
Divison of Electric Power Engineering
CHALMERS UNIVERSITY OF TECHNOLOGY
Gothenburg, Sweden 2021

Magnetically Biased Inductors in Switching Converters
Praveen Raju Hasbavi & Tejas Bharadwaj Prakash

© Praveen Raju Hasbavi & Tejas Bharadwaj Prakash, 2021.

Supervisor: Christoffer Levandowski, QRTech AB
Examiner: Torbjörn Thiringer, Chalmers University of Technology

Master's Thesis 2021
Department of Electrical Engineering
Electric Power Engineering
Chalmers University of Technology
SE-412 96 Gothenburg
Telephone +46 31 772 1000

Cover image: Typeset in L^AT_EX
Printed by Chalmers Reproservice
Gothenburg, Sweden 2021

Magnetically Biased Inductors in Switching Converters
Praveen Raju Hasbavi & Tejas Bharadwaj Prakash
Department of Electrical Engineering
Chalmers University of Technology

Abstract

The power electronic industry is striving to shrink the power converters in both weight and volume while still delivering excellent performance. One possible way of making the magnetic component in the converter smaller is to utilize the magnetic material to a greater extent. In the common buck or boost type converter, the material is not used as efficiently as it could be. By introducing a magnetic DC bias in the magnetic circuit of the inductor it could be possible to utilize the entire B-H curve of the magnetic material, this should in principle make it possible to make the inductor smaller.

This thesis focuses on designing the biased inductor with a permanent magnet and introducing the designed biased inductor in the boost converter and perform analysis and have a comparison with a boost converter having standard inductor. Designing of the standard inductor is performed in COMSOL and the design of the biased inductor is modelled keeping the designed standard inductor as a base model. The boost converter is operated in 25kHz frequency and works at 12V to 24V DC/DC conversion with a power rating at 24W.

It was found that the size of the biased inductor is reduced with a factor of four compared to the standard inductor and the weight is reduced to 35%. Furthermore, the efficiency of both the boost converter with the standard inductor and with the biased inductor is studied and it remained almost the same at 93%.

Acknowledgements

We are thankful to QRTECH and Chalmers University for providing us the support for the completion of this project.

We would like to thank our supervisor, Engineering Electronics Mechanical Eng, Carl Petersson, for his continuous support throughout this master thesis project. Furthermore, we would also like to extend our gratitude to our manager, Christof-fer Levandowski for his support and believing us throughout the program. Also,we would like to show our gratitude for Dennis Johansson and all the lab members in QRTECH helping and guiding us in every step and it was pleasure for us to be part of highly technical team and had a good learning experience.

We would like to thank our supervisor and examiner, Torbjörn Thiringer, for guid- ing us and giving his valuable feedback. Finally, we would like to thank our friends and family for all their support in completion of this thesis.

Praveen Raju Hasbavi & Tejas Bharadwaj Prakash, Gothenburg, 2021

Contents

1	Introduction	1
1.1	Background	1
1.2	Previous Work	2
1.3	Purpose	2
1.4	Scope	2
2	Theory	3
2.1	DC-DC Switching Converters	3
2.1.1	Classification of DC-DC converters	3
2.1.2	Step-up converter (Boost Converter)	3
2.1.3	Inductor Design Specification	4
2.1.3.1	Standard Inductor	4
2.1.3.2	Biased Inductor	5
2.1.3.3	Inductor saturation testing	7
3	Case set-up	9
3.1	Boost converter model requirement	10
3.2	Design of Standard Inductor	10
3.2.1	Core: Material and Design Selection	10
3.2.2	Number of turns	11
3.3	Design of Biased Inductor	11
4	Simulation Modelling	15
4.1	LTspice Modelling	15
4.2	Inductor Design Modelling	17
4.2.1	Standard Inductor - Design using COMSOL	17
4.2.2	Standard Inductor - Design using FEMM	18
4.2.3	Biased Inductor - Design using COMSOL	20
4.2.4	Biased Inductor - Design using FEMM	21
5	PCB Design and Modelling	23
5.1	Schematics in Altium software	23
5.2	PCB Layout	24
6	Hardware Testing of the Designed Inductor	27
6.1	Inductor saturation testing	27
6.1.1	Standard inductor saturation testing	27

6.1.2	Biased inductor saturation testing	28
6.2	Boost converter model operation	29
6.3	Boost converter output waveform	30
6.3.1	Inductor Current Waveform	30
6.3.1.1	Biased inductor Current Waveform analysis	31
6.3.2	Diode Current Waveform	32
6.3.3	Capacitor Current Waveform	32
7	Results and Discussion	35
7.1	Standard and Biased Inductor - Boost converter test results	35
7.1.1	Power Comparison	35
7.1.2	Loss Comparison	35
8	Conclusion	37
8.1	Future Work	37
8.2	Sustainable Aspects	38
8.3	Ethical Aspects	38
	Bibliography	41
A	Appendix 1	I

1

Introduction

1.1 Background

DC-DC power converters are widely used in switch-mode dc power supplies and electric drive applications. The input to these converters is an unregulated DC-supply from the rectified line voltage, and hence switch-mode dc to dc converters are used to convert unregulated dc input into a controlled dc output. The power electronic industry is striving to shrink the power converter in both weight and volume while still delivering excellent performance [2].

Inductors (magnetic component) are probably one of the heaviest and more voluminous components found in most power electronic converters. One possible way of making the magnetic component in the converter smaller is to utilize the magnetic material to a greater extent. This can be achieved by introducing a magnetic DC bias in the magnetic circuit of an inductor. According to different studies and analysis, there are different types of designs for magnetic DC biasing of an inductor adapting these designs accordingly to the required application of power electronic converter and this topic is one of the major interests to investigate [1].

The inductors used in DC applications produce a highly unbalanced magnetizing current. The load line is usually operate in the first quadrant and the energy storage capacity on the third quadrant is unused [3]. In order to increase the storage capacity, biased inductors use permanent magnets to produce a negative biasing flux across the core material and thus increases the energy storage capacity of an inductor.

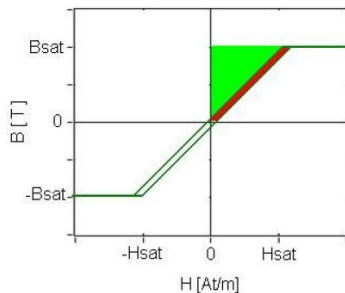


Figure 1.1: BH curve of Standard Inductor

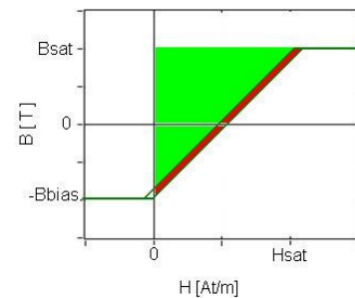


Figure 1.2: BH curve of Biased Inductor

1.2 Previous Work

A lot of research papers has been published for the development of inductors using biasing technique to reduce the core size and number of turns of an inductor [3]. The study has been made for the output filter of a DC-DC converter and it's efficiency is high compared to a standard inductor. However, we are using the same biased inductor for a high switching frequency DC-DC power converter and we analyze the losses and performance of both inductors.

1.3 Purpose

The main purpose of this thesis is to examine the possibility to reduce the core size and number of turns of an inductor by introducing permanent magnet to get a negative biasing flux, which is used in DC-DC power converters and analyzing the effect of losses and efficiency in comparison with the non biased inductor.

1.4 Scope

The scope of this project is to investigate, simulate, design, implement and test a switching power converter(boost or flyback) with a magnetically biased inductor and also have the comparison with a "standard" inductor power converter. A MOSFET is used as a switching component and the goal does not include the performance analysis with different switching components.

2

Theory

2.1 DC-DC Switching Converters

The switch mode DC to DC converters are used to convert an unregulated DC input into a controlled DC output at a desired voltage level. These converters are widely used in switch mode power supplies, the telecommunication sector and in the automotive sector. A block diagram of a DC-DC converter is shown in fig 2.1. It consist of an unregulated DC input voltage from a renewable energy source, DC-DC converter, load and controller. The controller acts as a negative feedback loop between the input voltage source and the Load. If the output load varies, then the controller helps the converter to provide the desired output voltage level by varying the PWM signal to turn ON and turn OFF of a switch.

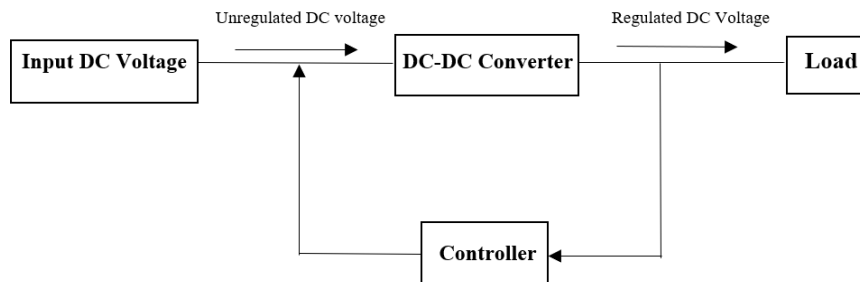


Figure 2.1: Block Diagram of DC-DC Converter

2.1.1 Classification of DC-DC converters

The switch mode DC to DC power converters are used to convert the unregulated Dc input into a controlled Dc output at a required voltage level. These converters are widely used in switch mode DC power supplies and in DC motor drives.

There are different types of DC-DC converters:

1. Step-down converter (Buck converter)
2. Step-up converter (Boost converter)
3. Step-down/step-up converter (Buck-boost converter)

2.1.2 Step-up converter (Boost Converter)

In this thesis we have used a step-up converter circuit to analyze the operation of the standard and biased inductor. The basic operation of the boost converter is to

step-up the output voltage compared to the input voltage. Figure 2.2 represents the circuit diagram of the step-up converter. When the switch is turned-on, the diode is reverse biased and all the energy is stored in the inductor, thus there will be no energy at the output from the input supply instead it receives energy from the capacitor. When the switch is turned off, the input energy and the energy stored in the inductor will flow to the output, thus the voltage across the output is more compared to the input.

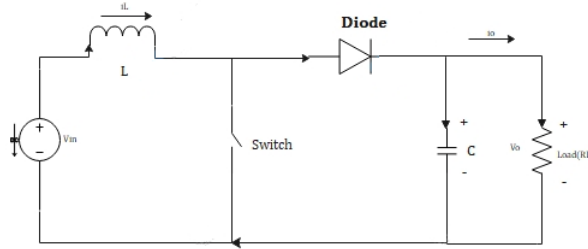


Figure 2.2: Step-up DC-DC converter

2.1.3 Inductor Design Specification

2.1.3.1 Standard Inductor

The initial step to design an inductor is to follow the design of the size to the required inductance and other operating requirements from the electrical circuit. To satisfy the requirement, (2.1) is followed. Equation (2.1) set the requirements to note such as magnetic saturation, area of cross-section and number of turns to avoid the exceeding more than the required sizing as well as considering magnetic saturation of the material. The LI product can vary with different design of the core and is mainly targeted to achieve different criteria like loss, size and cost [1]. From (2.1), the material is selected and its maximum operating flux density is determined and a specific design can be obtained from the data-sheet of the manufacturers,

$$LNI_{max} \leq LI = B_{Sat}NA_c \quad (2.1)$$

To fill the unknown like the number of turns, the reluctance of the air gap can be used from (2.2),(2.3) and the number of turns can be calculated as,

$$L_N = \frac{N^2}{R_g} \quad (2.2)$$

$$R_g = \frac{l_g}{\mu_0 A_g} \quad (2.3)$$

Introduction of the air gap is one of the major factors while designing the inductor since the material BH curve data has a specific saturation current and the linear region of the BH curve determines the inductors inductance. The Losses increase as the operating point of the inductor move towards the non-linear region of the

curve hence as we introduce the air gap the slope of the BH curve, increases which increases the saturation current thus reducing the risk of operating at the non-linear region as well as decreasing the losses.

As we determine all the required parameters (2.1) is checked if the selected parameters and the required LI is matching and tuned accordingly.

2.1.3.2 Biased Inductor

Biasing of the inductor with specific core shapes and introduction of the permanent magnet is studied and explained in many literature studies. Biasing of the inductor has its advantage for its increased energy storage capability and reduced size for the same standard/non-biased inductor topology.[1]

Following are the different types of biased core-based inductor which could be designed using the permanent magnet for biasing.

- PM inside air-gap
- PM near the air gap
- The saturation gap

As the name describes placing of permanent magnets and its operation studies are the criteria followed in each design. [1] and [3] describes these different types with its advantages and disadvantages. Due to the main advantages of the reduced core area and the number of turns to operate similar inductance topology of the non-biased inductor, the saturation gap biased inductor design is selected as our main design research area.

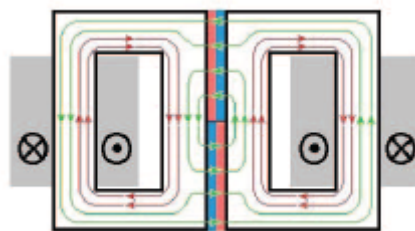


Figure 2.3: The Saturation-gap model

Figure 2.3 gives the example of the saturation gap design and its operation can be explained as follows.

From the research paper[5] the saturation gap gives the longest section for biasing flux from the permanent magnet and it induces a certain magnetic saturation point in the core, which acts as an air gap when compared with the non-biased inductor.

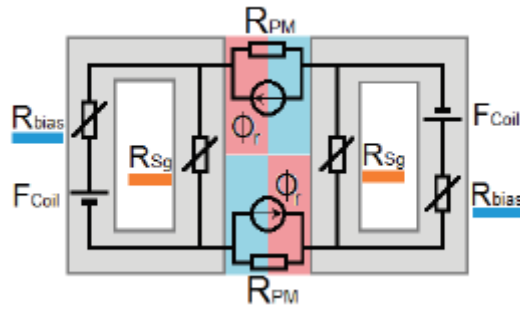


Figure 2.4: Magnetic Equivalent Circuit(MEC)

Design of saturation gap.

To understand the reluctance flux and the operation of it, the magnetic equivalent circuit (MEC) is created. From figure 2.4, R_{bias} is the reluctance of the biased core, R_{sg} is saturation gap reluctance and R_{PM} is the reluctance of the permanent magnet.

Since biasing of the inductor take place by introducing a PM, the BH curve operation of the biased inductor will have different operation modes.

- Sub-saturated mode
- Full linear bias
- Over-Saturated

Since our operational inductance is desired to have its operating point in a linear region of the BH curve to have a constant inductance for the electrical circuit design requirement. So, full linear bias mode is used in our designed inductor.

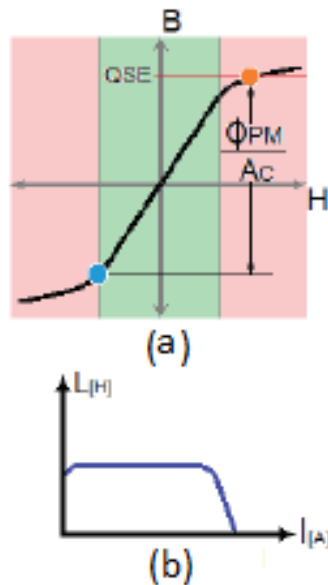


Figure 2.5: Full Linear Bias mode, (a) The operational BH curve characteristics, (b) LvsI profile

Full linear bias mode is the operational design characteristics chosen to operate the inductor in the linear region of the BH curve as shown in the figure 2.5.

Quasi-Saturated Equilibrium (QSE) is defined to be the operational flux density limit achieved in any given point on the core and saturation gap flux density, R_{sg} is set to the QSE value so that the operation will be in its linear mode. The choice of the QSE value is defined according to the material linear property and chosen to be between 150% to 200% of the maximum saturation flux density of the material.

As we can understand, in the standard inductor the design specification the flux density is 0T when the current is at 0A. But during the biased full linear mode, the flux density at 0A, the saturation gap will be at QSE value but the flux density at 0A of the biased core will be in the third quadrant, since the main goal is to increase the energy storage capability. As the current increase in the coil, the flux density moves towards the first quadrant, since the aim is to keep the inductance constant the strength of the permanent magnet reduces to keep the saturation gap flux density at the QSE value. Thus the operation of full biased mode works.[3]

2.1.3.3 Inductor saturation testing

Saturation is the point where the core of the inductor operation moves from the linear region of the BH curve operation to the non linear region operation point. So, Testing inductor saturation is a verification of the designed setup. Figure (2.6) gives the testing setup carried to understand the saturation current. When constant voltage(E) is applied across the inductor, the current will increase with respect to time, following the $I=E*t/L$ and by measuring the current waveform the saturation current can be determined. The figure 2.6 is modified to figure 2.7 to reflect high the current operation and measuring of the high current. The rig setup will be explained in section(6.1).

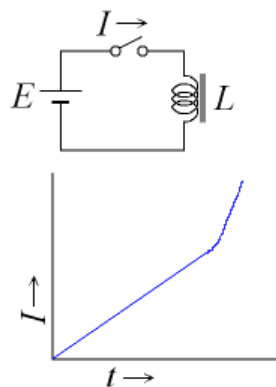


Figure 2.6: Generalised circuit to measure inductor saturation current

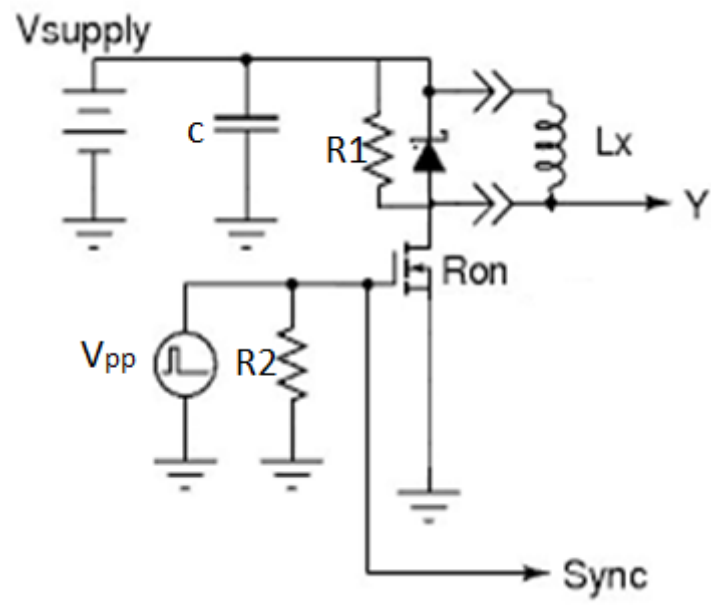


Figure 2.7: Inductor saturation current scheme

3

Case set-up

Reference	<ul style="list-style-type: none">• Literature study to understand the biasing methods and topology• Selecting boost converter as the primary analysis converter for the study of the inductor
LTspice Simulation	<ul style="list-style-type: none">• Design and calculation of the boost converter to design a required inductor• Specification to design inductor: $V_{in}=12V$, $f_{sw}=25kHz$, $I_L=2.1A$ and $I_o=1A$
Design of standard Inductor	<ul style="list-style-type: none">• Design of a standard inductor of 390uH for the boost converter operation• Simulation in COMSOL and FEMM with the design parameters and specifications
Design of Biased Inductor	<ul style="list-style-type: none">• Use the same design parameter as a base model to bias the inductor and alter\reduce its core dimension and number of turns
Selection of Components	<ul style="list-style-type: none">• Components such as core, a permanent magnet for designing of the inductor• Controller such as Arduino nano is used to analyse the output performance• Ultra low on-resistance switching transistor is selected for better output-IRFZ44NPBF
Hardware Model	<ul style="list-style-type: none">• Building of the component in the breadboard to finalize the design and understand the operation of the circuit
PCB Design	<ul style="list-style-type: none">• Altium software is used for building schematics and PCB layout
Testing and Analysis	<ul style="list-style-type: none">• Testing of the PCB model with the component will be carried out

Figure 3.1: Overview of the thesis work

3.1 Boost converter model requirement

The Design parameters of a simple boost converter is shown below:

Given: Input voltage = 12V,

Output voltage= 24V,

Efficiency = 100%,

Switching frequency = 25kHz,

Power= 25W,

Output voltage ripple= 1%,

Output current ripple= 30%.

$$DutyRatio : D = (1 - \frac{V_s}{V_0})\eta = 1 - \frac{12}{24} * 1 = 0.5 \quad (3.1)$$

$$Inductance : L \geq \frac{V_s(min)D}{f_s \Delta I_L} \geq 384\mu H \quad (3.2)$$

$$Capacitance : C \geq \frac{I_0(max)D}{f_s \Delta V_c} \geq 86.7\mu F \quad (3.3)$$

$$Load : R = \frac{V^2}{P} = 24\Omega \quad (3.4)$$

3.2 Design of Standard Inductor

The design of the standard inductor is carried out in this study. From (2.1), the selection of the core material and core design is carried out in COMSOL and FEMM softwares. which uses the finite element method for the analysis of the magnetic path and studied under magneto-static analysis.

3.2.1 Core: Material and Design Selection

As the design of the inductor is for a high-frequency application ferrite core is used, so that it can withstand an external magnetic field, hysteresis and has a low operational loss. B_{sat} plays an important role since the same design is included in the biasing, hence N series Ferrite material had suitable maximum B_{sat} in linear operational mode. This thesis work focuses on the study of the N27 material with $B_{sat}=0.5T$.

Now a selection of the core design according to the (2.1) requires the calculation to satisfy the LI characteristic. Hence taking the selected material N27 the area of the cross-section is selected to be $432mm^2$. The core shape consists of the 8-U shape core arranged as a two E shape plane. The reason for the selection of the specified design, since the reduction of core and creating the saturation gap design can be possible by choosing as U shaped core. The selected core has a dimension of $25*20*13mm$.

3.2.2 Number of turns

This section defines the calculation of the total number of turns. The selection of the core size and shape of the window area, fill factor(K_u) and coil dimension should be considered. As explained earlier, the introduction of air-gap play a vital role. So, from (2.2) and (2.3) the total number of turns required can be calculated to be $N=42$.

The window area could be available from the core design parameter and the fill factor is assumed to be 0.6. Hence a total number of turns of 42 can be fitted by using 2 layers of 21 turns each. Using multi-layers is an advantage for high frequency and for a power application, since it reduces losses when compared to the single-layer winding.[4]

Figure 3.2 give the BH data of the N27 material. Table 3.1 tabulate the required parameter for the design of standard inductor.

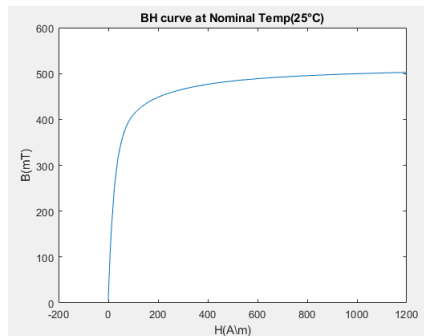


Figure 3.2: BH curve of N27 ferrite material in first quadrant

Table 3.1: Design parameters of standard inductor

Material	N27 Ferrite core
B_{sat}	0.5T
Core dimension(L*H*B)	50mm*40mm*27mm U core
Area of cross section(A_c)	432mm ²
Number of turns	41
Window area(W_c)	216mm ²

3.3 Design of Biased Inductor

The design of the biased inductor is performed on the standard inductor and considered to be the base model. Hence, the core material and the design is similar to the standard inductor, but the main aim is to reduce the core dimension. Equation (2.1) changes, as we need to reduce the area of core cross-section A_c we modelled to reduce 4 times and the reduction of the core size increases the losses by twice[1]

but the total loss is so low that the twice of it doesn't make a significant effect on the design of the inductor.

$$LI = L_N(I_{max} - \frac{F}{N}) = B_{Sat}NA_c \quad (3.5)$$

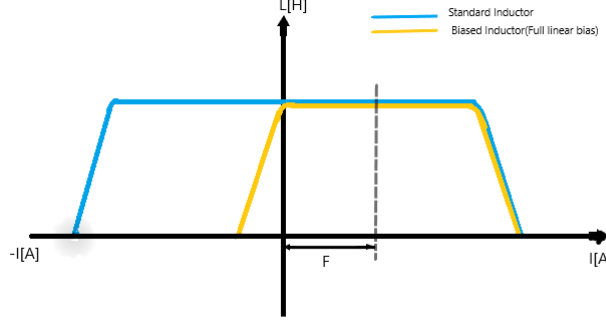


Figure 3.3: LvsI profile of standard inductor and Biased inductor with effect of permanent magnet magnetizing force(F)

From (3.5), the F/N factor will be introduced in the design since the introduction of the permanent magnet take place. Since in the operation, we desired to be in full linear mode, the F/N characteristic would be equal to the $I_{max}/2$. Where F is the magnetizing force due to the introduction of the magnet. The magnetizing force play a vital role in increasing the saturation point at the F point as shown in figure 3.3. Hence it is assumed to be $I_{max}/2$ for the design of the Biased inductor.

Introducing PM flux is the next step procedure.

Defining the PM flux at 0A is defined by PM material remanence (B_r) and area of the cross-section (A_c) of PM. This can be calculated using(3.6),(3.7).

$$\Phi_{PM} = A_{PM}B_r = A_c(B_{bias} + B_{sg}). \quad (3.6)$$

$$R_{PM} = \frac{l_{PM}}{\mu_0\mu_r A_{PM}} \quad (3.7)$$

Since the operation is in full linear bias mode where B_{sg} has a QSE value which is equal to 200% of B_{sat} and B_{bias} is material maximum saturation flux density. Hence selection of remanence should not operate the material at non-linear mode at 0A and hence B_r is chosen to be 0.35T. Using (3.6) and (3.7) the required A_{PM} is calculated and is 470 mm^2 . The required A_{PM} available in the market but a suitable close area is considered and its area is of 520 mm^2 hence inductance can be kept constant using the number of turns. A number of turns can be calculated using (3.8) since the market available area of PM and flux is defined, the number of turns can be altered to get the required inductance L_N .

$$L_N = \frac{N^2}{R_{PM}} \quad (3.8)$$

Hence the number of turns $N=25$ for a single limb. Table 3.2 tabulate the required

parameter for the design of biased inductor.

Table 3.2: Design parameters for biased inductor

Material	N27 Ferrite core
B_{sat}	0.5T
Core dimension(L*H*B)	58.5mm*40mm*13mm U core
Area of cross section(A_c)	$432/4 = 108\text{mm}^2$
Number of turns	25(at each limb)
Window area(W_c)	104mm^2
Magnetic material	N35(NdFeB)
$B_r(PM)$	3550G (surface gauss)
Area of PM	520mm^2
PM dimension(L*B*H)	6.5mm*13mm*20mm
Magnetization path	Axial

4

Simulation Modelling

4.1 LTspice Modelling

The best way to analyze or understand the operation of any electrical circuit is by performing a simulation under various electrical conditions. To simulate, the LTspice software is user-friendly, it provides the details of the components which are available in the market and also gives the waveform to understand and analyze the output of an electrical circuit. In this simulation, the performance of 12V to 24V boost converter using MOSFET as a switch. The switching and other conduction losses are neglected in the calculation.

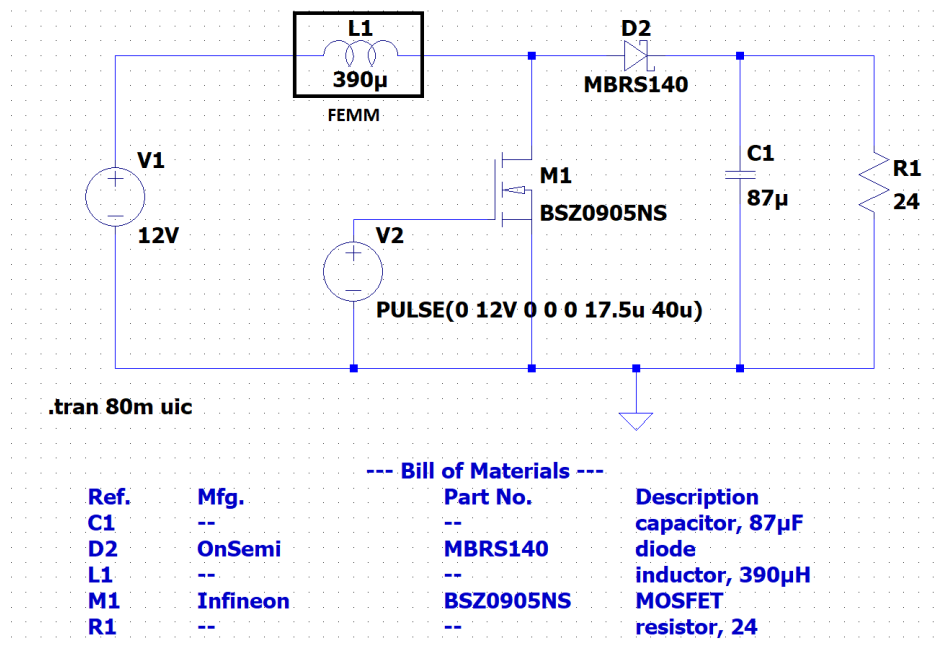


Figure 4.1: 12V to 24V Boost Converter circuit in LTspice

4. Simulation Modelling

For the switching purpose, a N-channel MOSFET (BSZ0905NS) is used in the LTspice simulation. Due to the non-availability of PWM IC-LM3842 in the LTspice library, a pulse width voltage source with an on-time (T_{on})= 17.5micro sec, Total time period(T_{period})= 40micro sec is used. For the forward biasing operation of the boost converter, the Schottky diode (MBRS140) with an average forward current of 1A and a breakdown voltage of 40V is used. The overall schematic diagram is shown in figure 4.1. The input and output voltage is shown in figure 4.2. The initial spike in the voltage is due to a sudden inrush of current while switching on and off. Figure 4.3 shows the current across an inductor and the load current. By looking at the output wave-forms, we can say that our boost converter is working as expected.

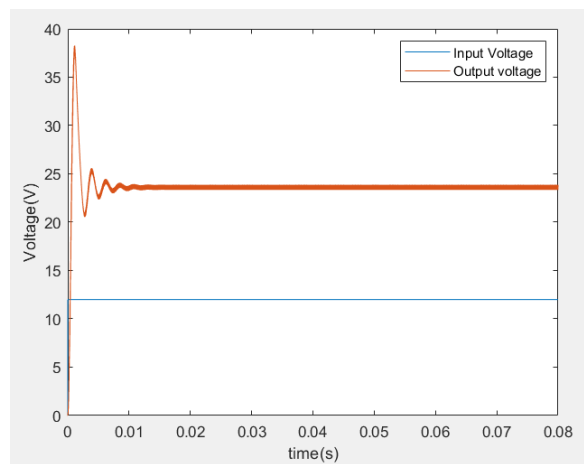


Figure 4.2: Input and Output Voltage waveform

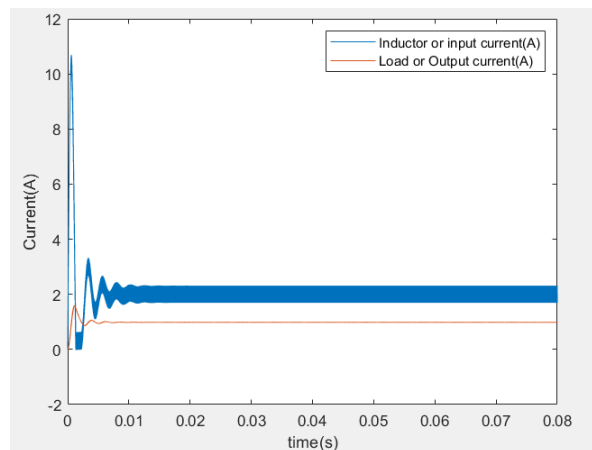


Figure 4.3: Input and Output Current waveform

4.2 Inductor Design Modelling

4.2.1 Standard Inductor - Design using COMSOL

The figure 4.4 gives the design of the standard inductor in 2D analysis COMSOL multi-physics, where a finer mesh node is created. The depth is defined as required which is 27mm^2 .

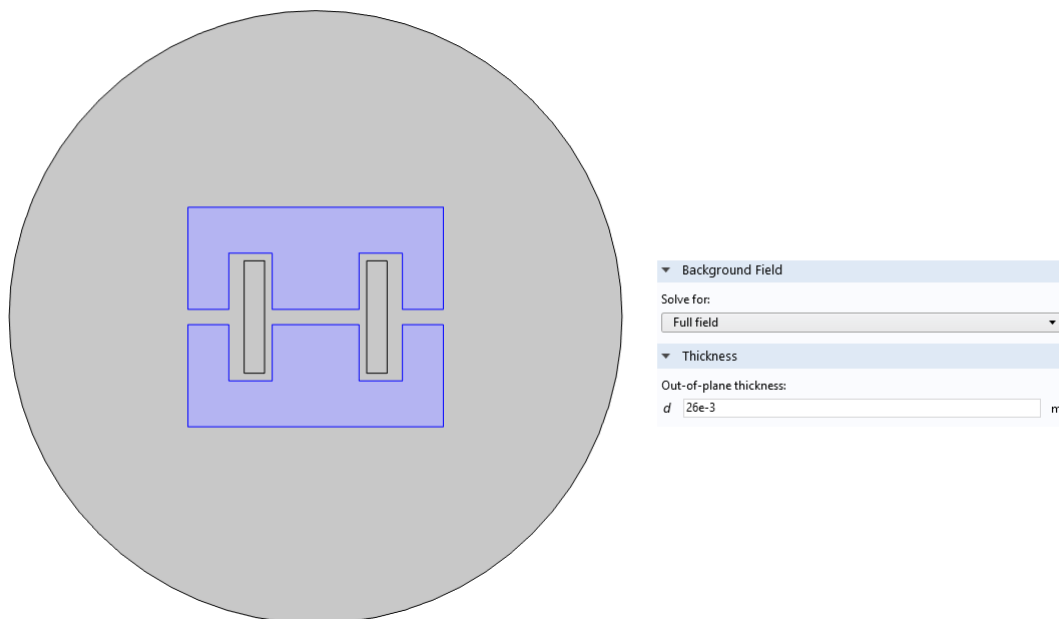


Figure 4.4: Design layout of standard inductor in COMSOL

Using the Magneto-static analysis with current a rating of 2.1A and total number of turns is 45, the inductance obtained in COMSOL is $350\mu\text{H}$. The study is carried out with coil geometry and stationary analysis having N27 material BH data and coil dimension of 1.2mm2 diameter. Below the result explains the flow of flux direction, flux density and the given point on the core material. The flux density at any given point does not get saturated when operated at our operating current of 2.1 A and the maximum flux density is 0.25 T at corner. Even though the calculated number of turns is 41 but the number of turns used while simulation is 45. This slight change is due to that, we have neglected the effect of flux at the corner and not taken fringing effect into the calculation. Due to that the change in number of turns is observed.

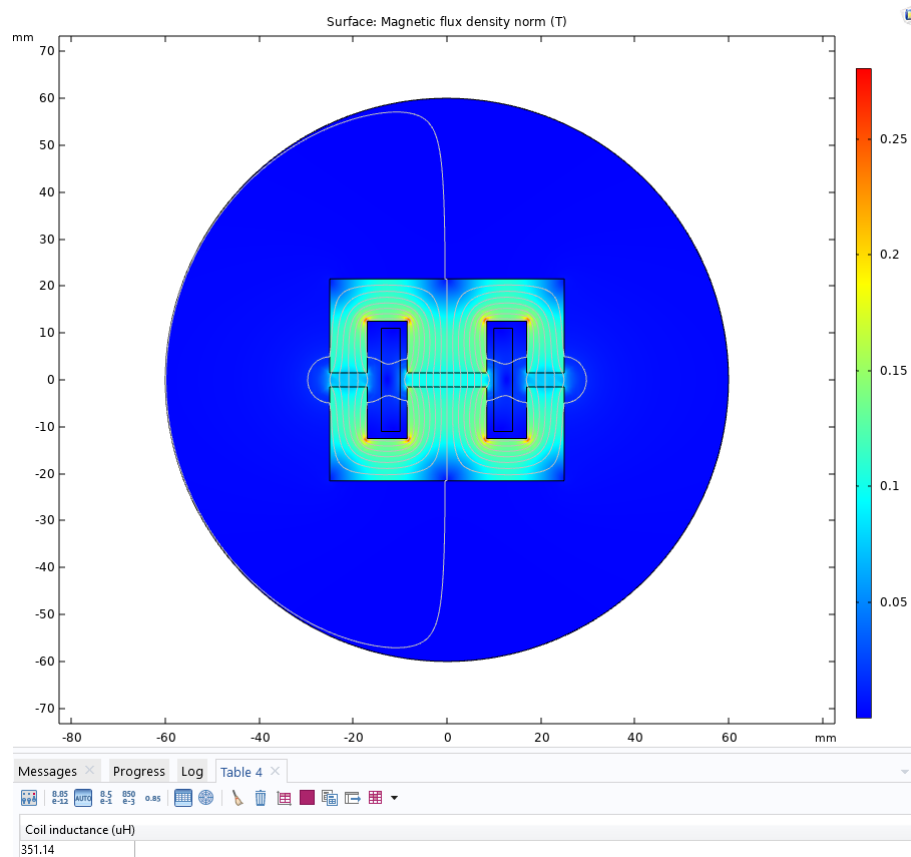


Figure 4.5: Flux density and flux path result of standard inductor in COMSOL

4.2.2 Standard Inductor - Design using FEMM

Design of the COMSOL and analysis of the software is supported or verified using FEMM software and the figure 4.10 shows the same dimension parameters used as in COMSOL

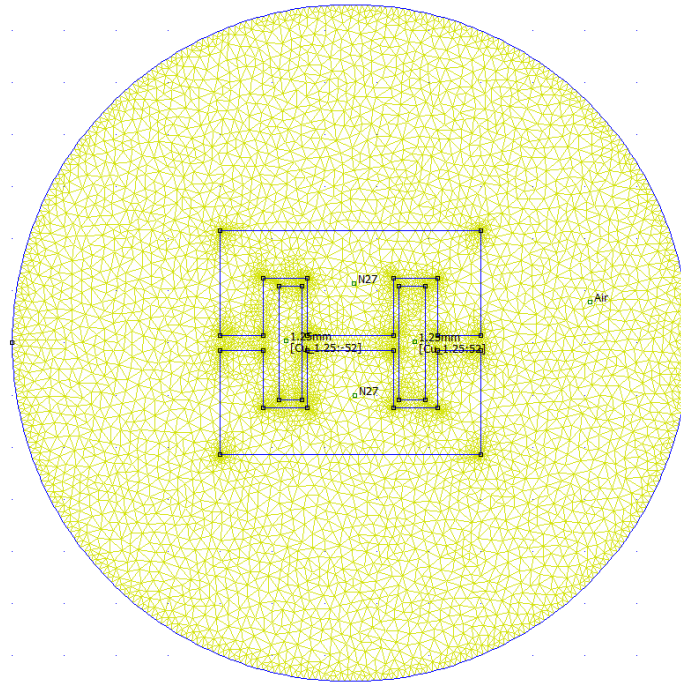


Figure 4.6: Design layout of standard inductor in FEMM

From the figure 4.7 the result is explained in flux/current which is referred to as inductance and its matching the COMSOL result of $350\mu\text{H}$.

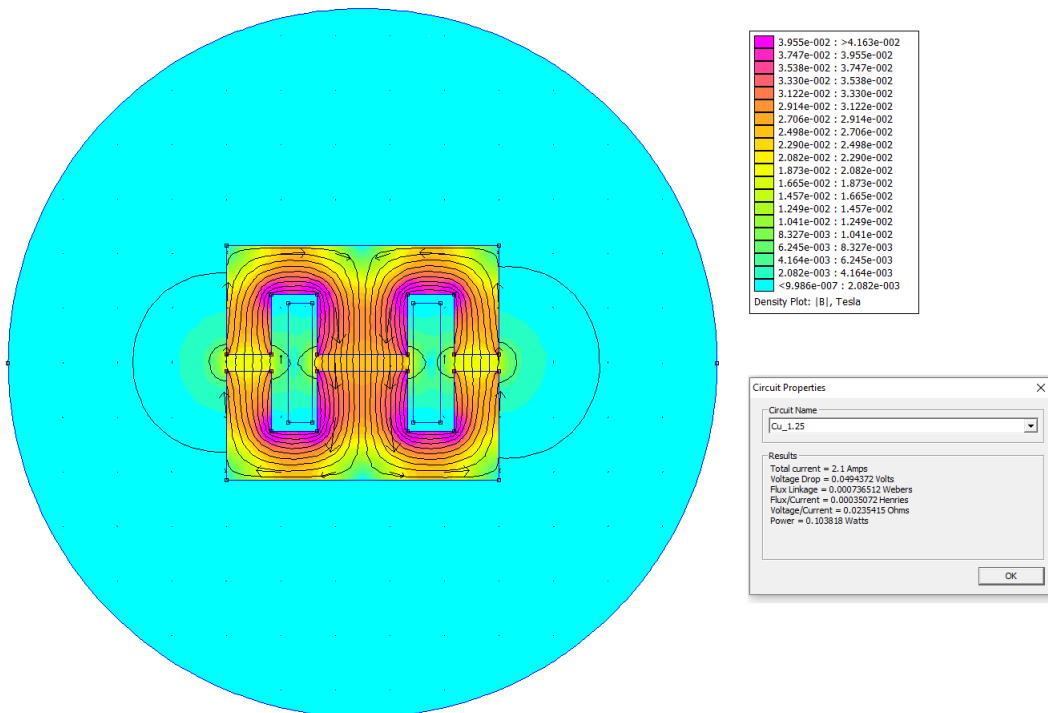


Figure 4.7: Flux density and flux path result of standard inductor in FEMM

4.2.3 Biased Inductor - Design using COMSOL

Below is the design layout of the biased inductor and analysis is carried out in magneto-static analysis. Where the middle two rectangular box defines to be a Permanent magnet with required remanence and 2D analysis is carried out with a depth of 13mm since it defines the reduced core. The length between the permanent magnet is altered to get the desired inductance since the calculation does not include the non linear behavior of the PM and is adjusted to get the desired inductance.

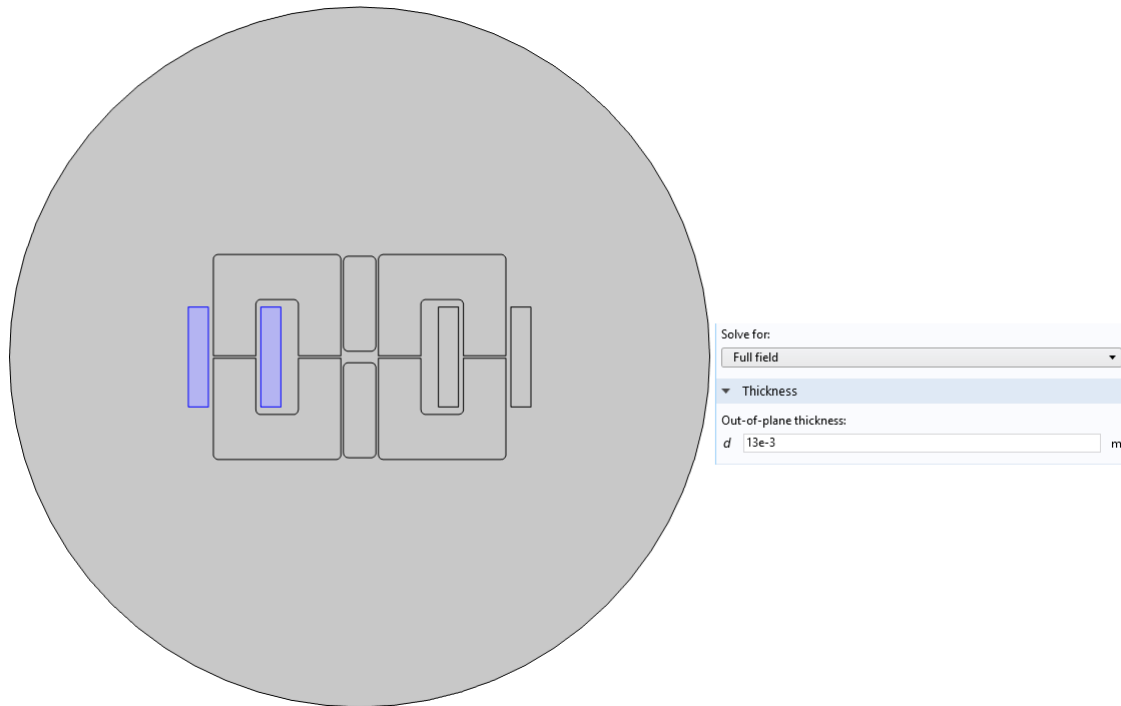


Figure 4.8: Design layout of Biased inductor in COMSOL with permanent magnet

The result of flux density and flux path is given in figure 4.9. The result obtained at each limb was $400\mu\text{H}$ and the core does not get saturated and operate below the maximum saturation flux density of 0.5T when operated at a maximum current of 2.1A.

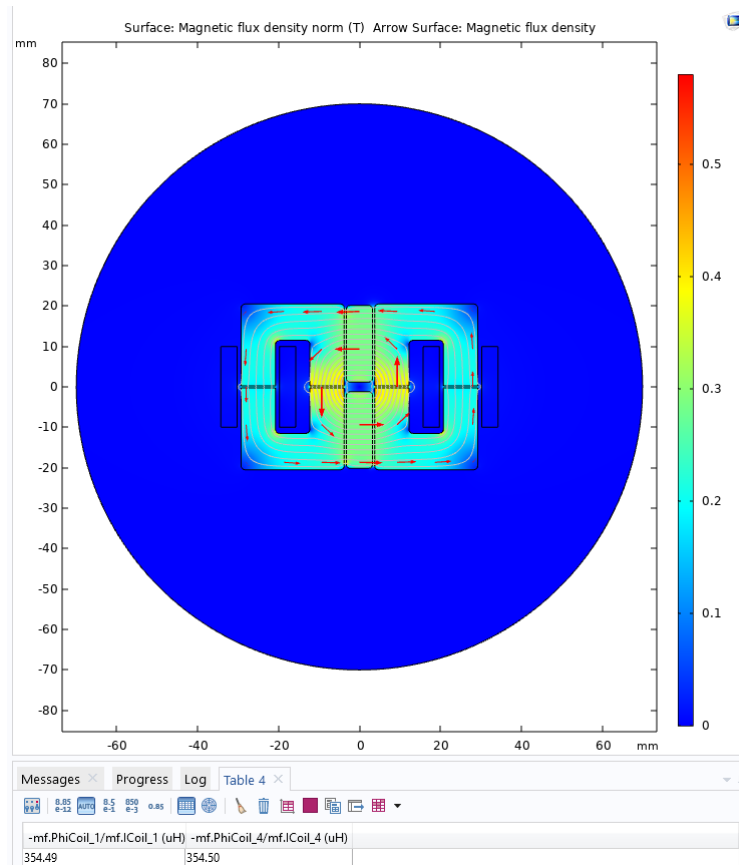


Figure 4.9: Flux density and flux path result of Biased inductor in COMSOL using permanent magnet

4.2.4 Biased Inductor - Design using FEMM

The design of COMSOL and analysis of the software is supported or verified using FEMM software and figure 4.10 shows the same dimension parameters used as in COMSOL using the same depth of 13 mm.

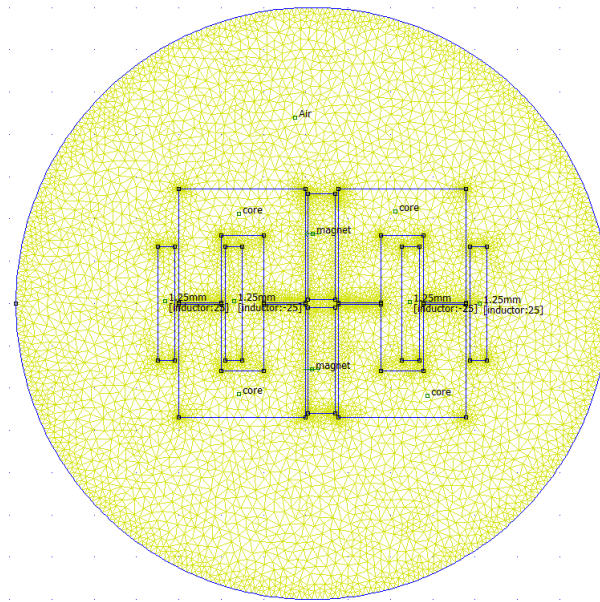


Figure 4.10: Design layout of Biased inductor in FEMM

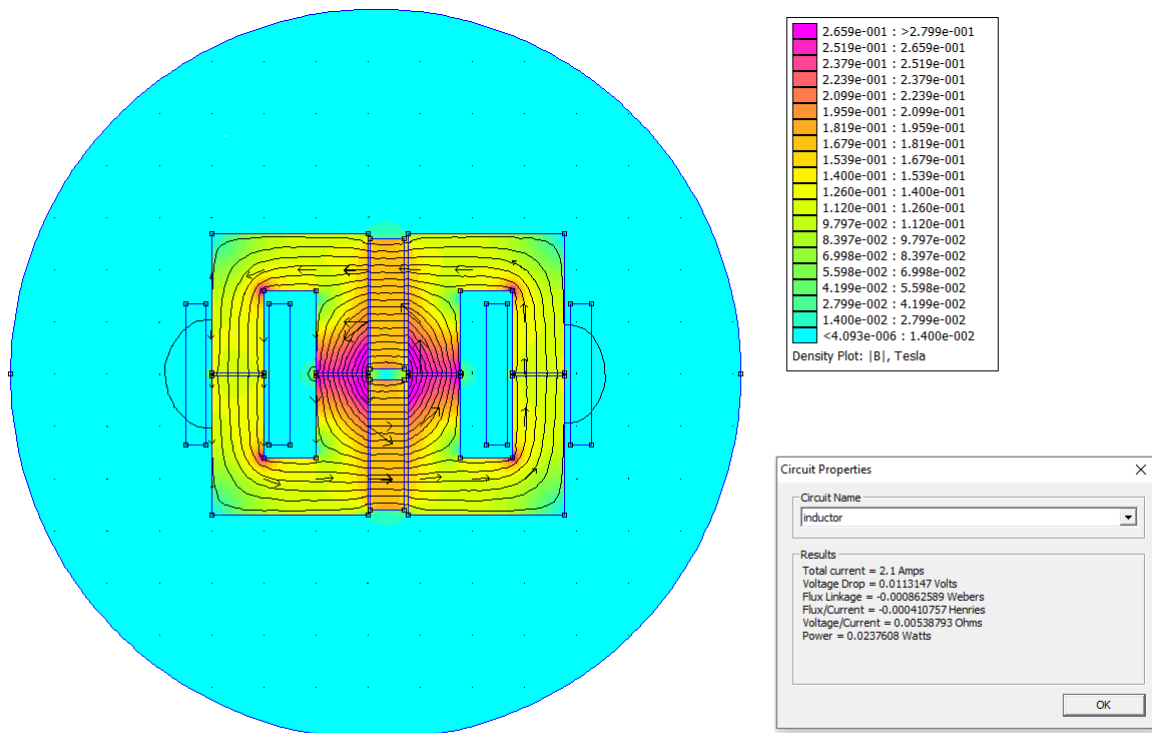


Figure 4.11: Flux density and flux path result of Biased inductor in COMSOL using permanent magnet

5

PCB Design and Modelling

The schematic and PCB design of a DC-DC boost converter circuit is discussed in this section. The PCB designing is carried out using the Altium software.

5.1 Schematics in Altium software

Altium is a software used for the design of a DC-DC boost converter circuit. After analyzing the performance of the DC-DC boost converter in the LTspice simulation, the hardware implementation of the boost converter circuit is carried out. Based on the PCB layout requirement the production file is generated.

In the PCB schematic, two connectors are used to connect the input power and output load. Two separate PCB designs are carried out for the standard inductor and the biased inductor as shown in figure 5.1 and figure 5.2. The IRFZ44NPbF N-channel MOSFET is used as a switch for the boost converter. To control the gate pulse of a MOSFET, the ARDUINO NANO is used. By varying the potentiometer(100k) a constant frequency of 25kHz and duty cycle 0.5 is adjusted. The input power to the ARDUINO is provided by the LM7808 voltage regulator, which regulates the 12V input to the 8V output. The Capacitance of 0.33 μ F is connected across the input and output of the LM7808 voltage regulator, the input capacitor (C_{in}) is required if the regulator is located at an applicable distance from the power supply filter and the output capacitor (C_0) is needed to improve transient response. To control the reverse flow of current, the surface-mounted MBRS140 forward bias diode is used in the schematic. At the output stage the bulk capacitor of capacitance 100 μ F and 50V is used to store the energy. All the footprints of components used in the PCB schematic are created using the available QRTECH AB - Altium Library. The surface mounted resistor and capacitors are selected with the 0805 component size. Altium provides an electrical rule check, which checks for short circuit connection or any missing paths. After verification, all the required data for the supplier is generated in the form of a netlist.

5.2 PCB Layout

The PCB layout design is carried out for the implementation of the hardware design. For our design we have used a four-layer PCB with different copper thickness, which is shown in table 5.1. Different parameters like width of the track, via diameter, Clearance, etc., are considered while designing. The values for different parameters is shown in table 5.2

Table 5.1: PCB Layers

Layers	Type	Material	Thickness
Top Layer	Cu layer + Solder resist	FR-4	10 μ m
Layer 1	Copper layer	FR-4	35 μ m
	Prepreg		78 μ m
Layer 2	Copper layer	FR-4	1.2mm
Layer 3	Copper layer	FR-4	78 μ m
(GND)	Prepreg		78 μ m
Layer 4	Copper layer	FR-4	35 μ m
Bottom layer	Cu layer + Solder resist		10 μ m
Total PCB thickness			1514 μ m

Table 5.2: Design parameters for PCB layout

Parameter	Value
Minimum track width	1.2mm
Minimum via diameter	1.27mm
Minimum solder mask width	0.010mm
Minimum clearance	175 μ m

These parameters is imported for the designing of the PCB. The total PCB board dimension is 156.99mm x 24mm. Once the PCB design is complete, the relevant Gerber files and files related to the footprint position on top and bottom layer of the PCB are generated for the production. Figure 5.1 and 5.2 show the PCB view of the standard inductor - Boost converter and Biased inductor - Boost converter.

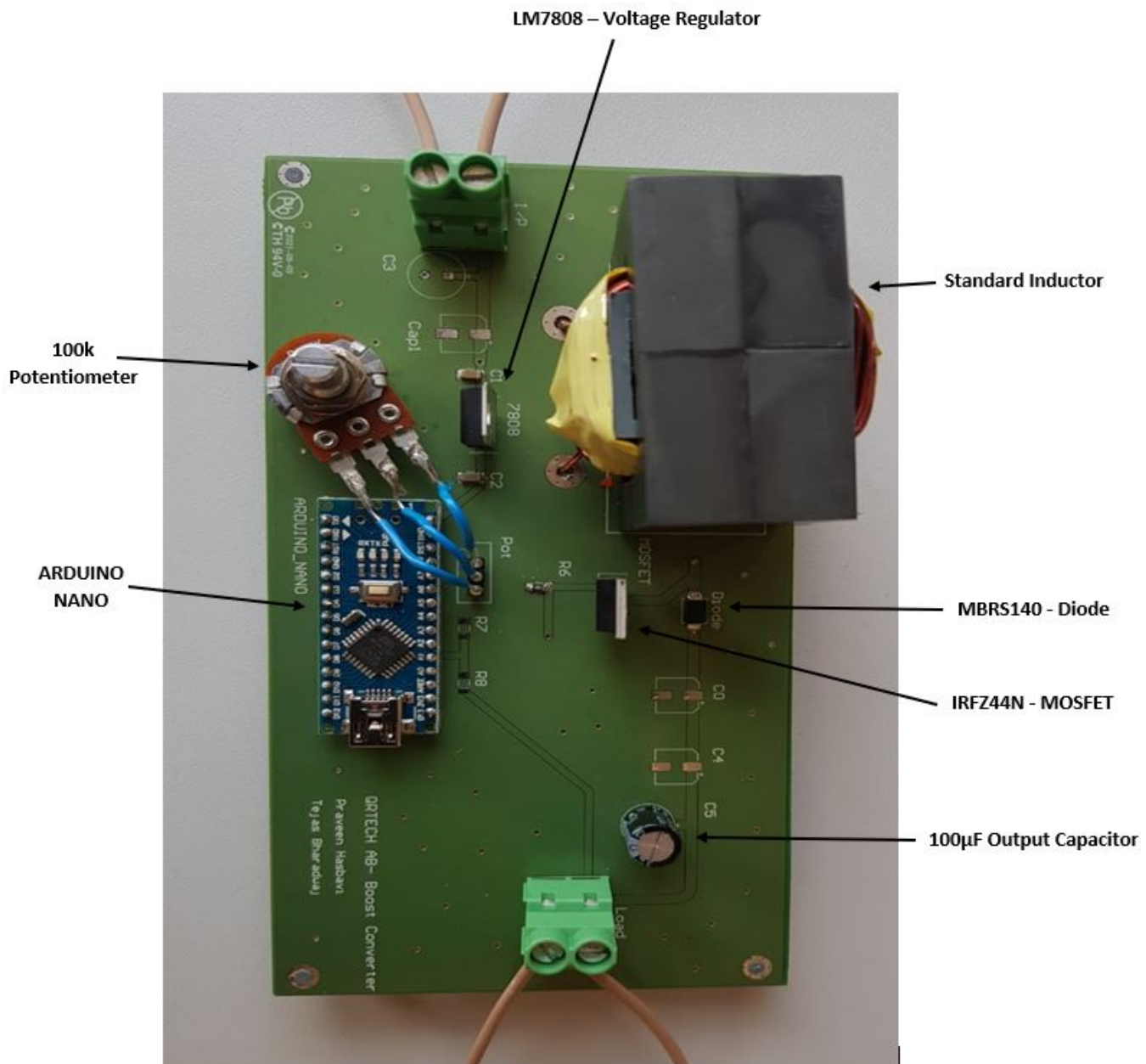


Figure 5.1: Standard Inductor - Boost Converter PCB Design

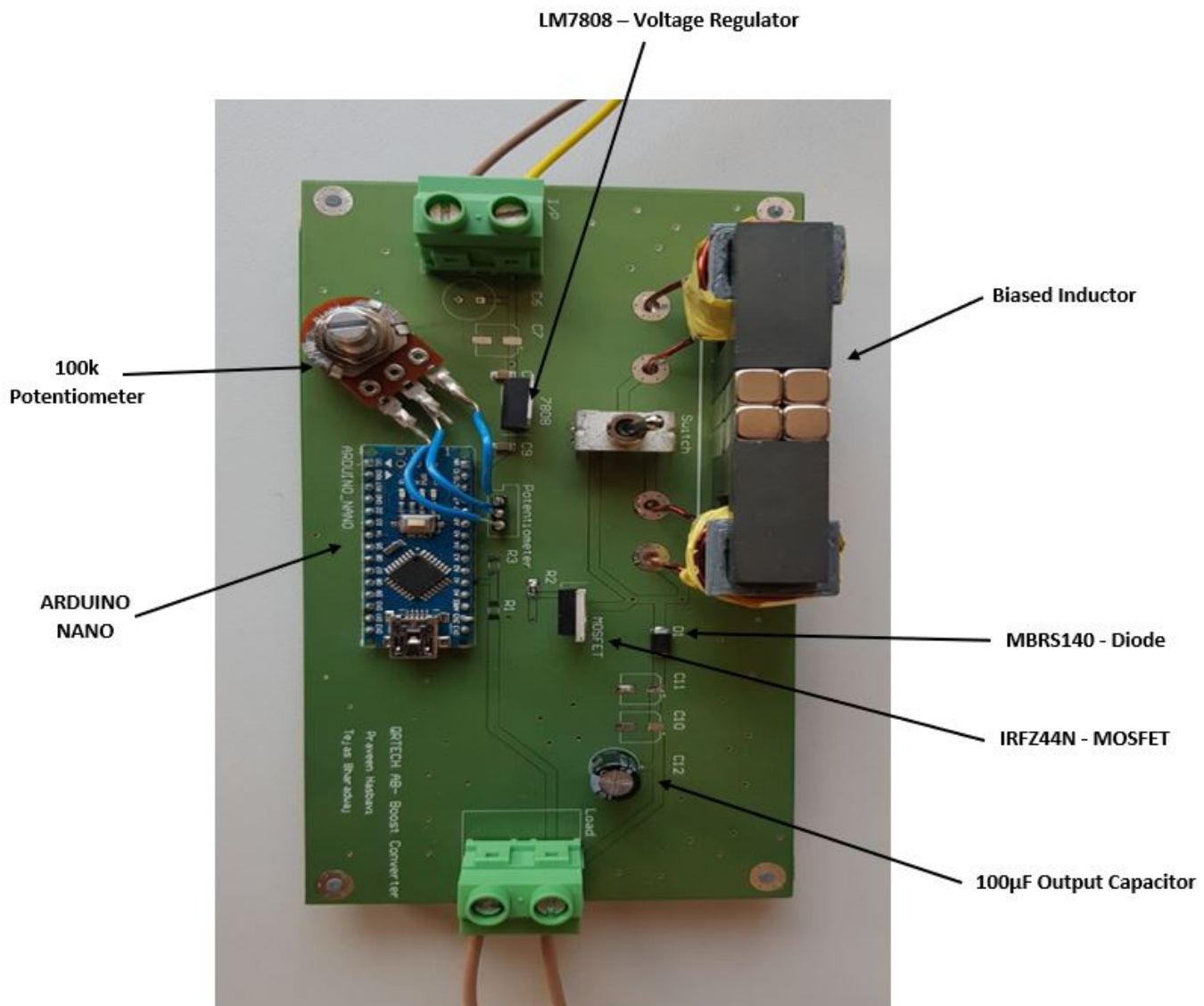


Figure 5.2: Biased Inductor - Boost Converter PCB Design

6

Hardware Testing of the Designed Inductor

6.1 Inductor saturation testing

Testing of inductor saturation current performance is to analyse the operation of the inductor and test its peak current operation point and its ability to give the designed inductance to the circuit. The Inductor saturation test explained in section (2.1.3.3) could determine the peak current operation and waveform analysis will determine its capability to operate with the designed inductance and having the designed peak current. Figure 2.7 can be set up as shown in figure 6.1. The MOSFET is operated at 10KHz, controlled by the arduino and the supply is supported by charging and discharging a capacitor bank of 200uF. The current is sensed across the inductor using current sensor to determine the saturation a current of the inductor.

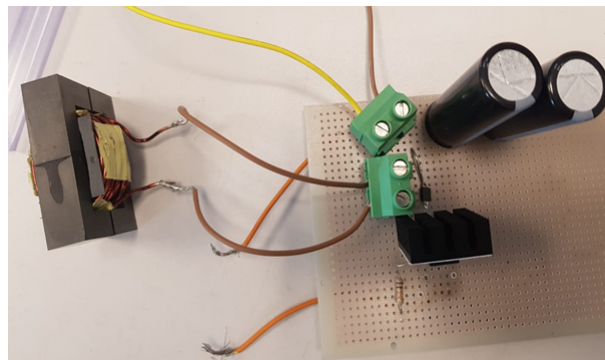


Figure 6.1: Testing setup for measuring saturation current

6.1.1 Standard inductor saturation testing

Figure 6.2 gives the waveform of the saturation knee point of the standard inductor. Figure 6.3 gives out the analysis of the simulation knee point for the saturation current. This proves to be approximately matching with theory at 14A.



Figure 6.2: Test Result for measuring saturation current

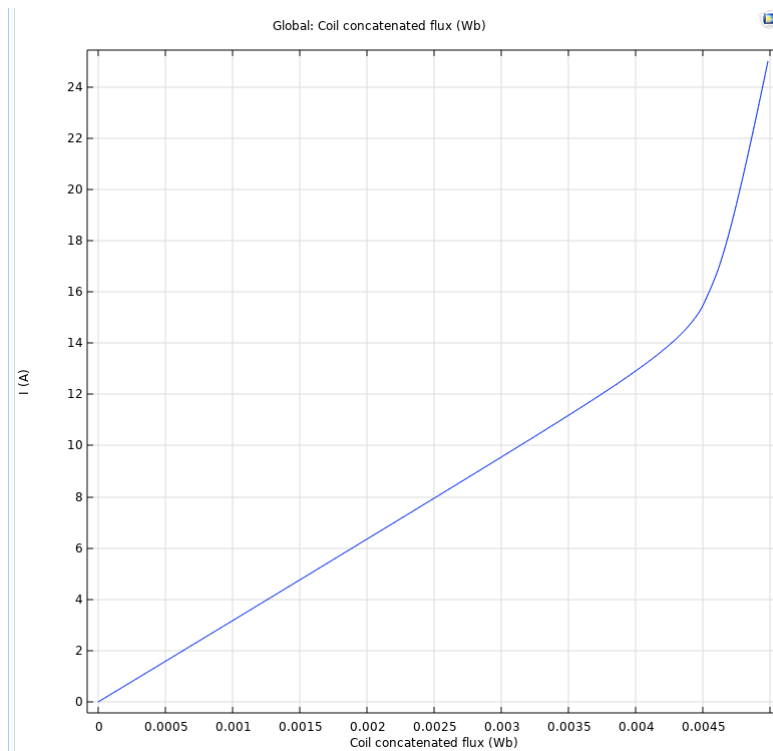


Figure 6.3: Simulation result for measuring saturation current

6.1.2 Biased inductor saturation testing

Figure 6.4 gives the waveform of the saturation knee point of the standard inductor. Figure 6.5 gives out the analysis of the simulation knee point for the saturation current. This proves to be approximately matching with theory at 15A.

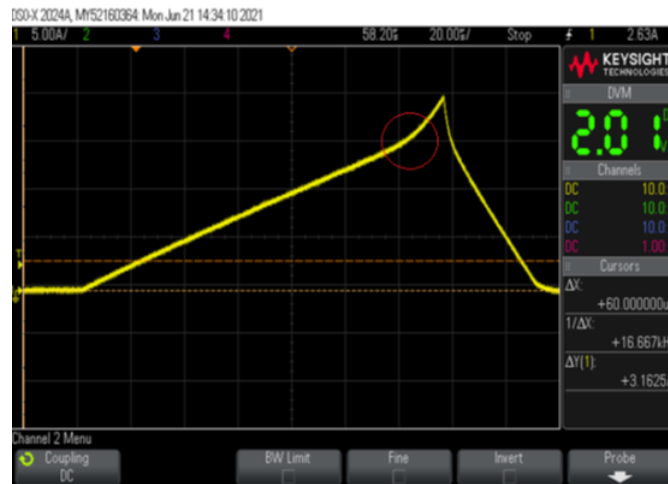


Figure 6.4: Test Result for measuring saturation current

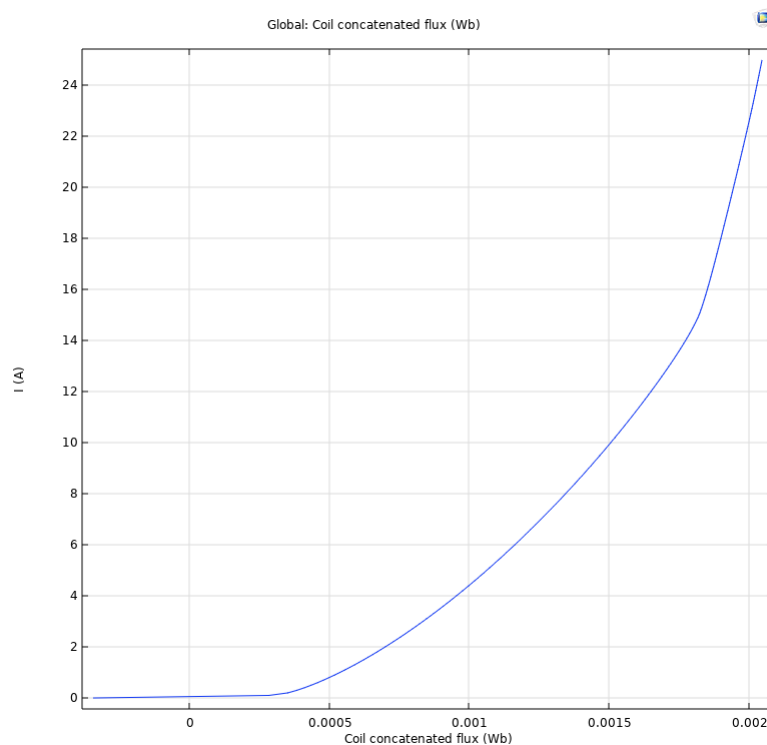


Figure 6.5: Simulation result for measuring saturation current

6.2 Boost converter model operation

The boost converter operation is analysed based on the design of the converter as explained in section (2.1), the output and input is compared with the model and it can be verified from the model's output. The designed PCB model given in figure 6.6 and figure 6.7 gives the desired output since the input 12V and expected output is 24V which can be seen the figure. The loss analysis will be explained in

6. Hardware Testing of the Designed Inductor

section(reference).In the model aurduino nano is the controller which operates in 25kHz as designed and duty cycle is assigned by the potentiometer.

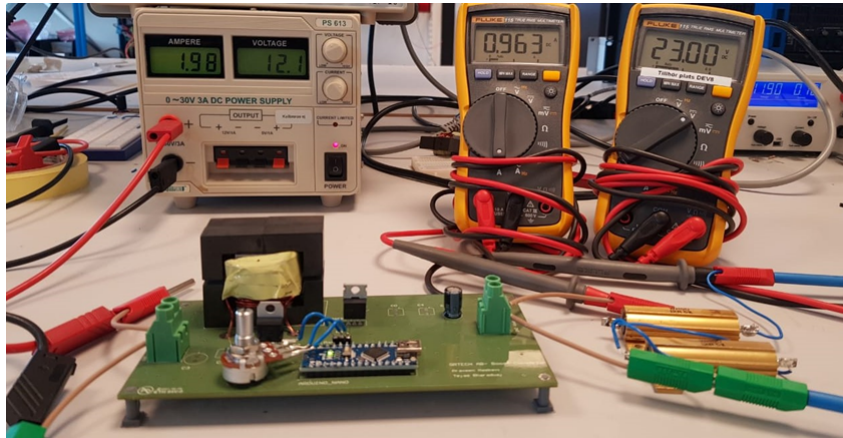


Figure 6.6: Standard Inductor Boost Converter

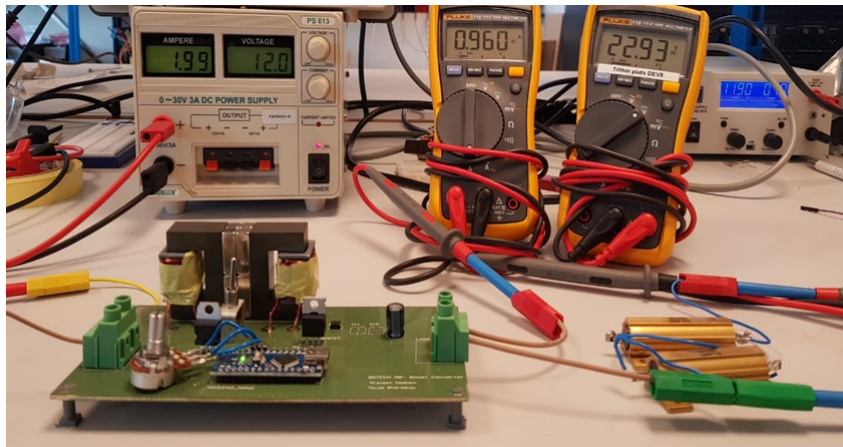


Figure 6.7: Biased Inductor Boost Converter

6.3 Boost converter output waveform

6.3.1 Inductor Current Waveform

Inductor current waveform is the initial analysis to verify the boost converter operation since the initial component connected to the input is inductor and also it act as energy storage device.Based on the theory the waveform is expected to be triangle charging when the mosfet is turned on and discharge when the mosfet is turned off.Figure 6.13 gives the current waveform of standard inductor with measured current ripple to be 0.73A and figure 6.14 gives the waveform of the biased inductor with measured current ripple to be 0.76A which is as expected and explained in case set-up.

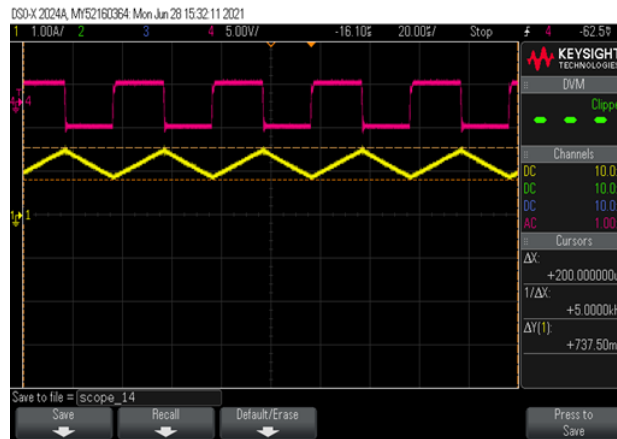


Figure 6.8: Standard inductor current waveform

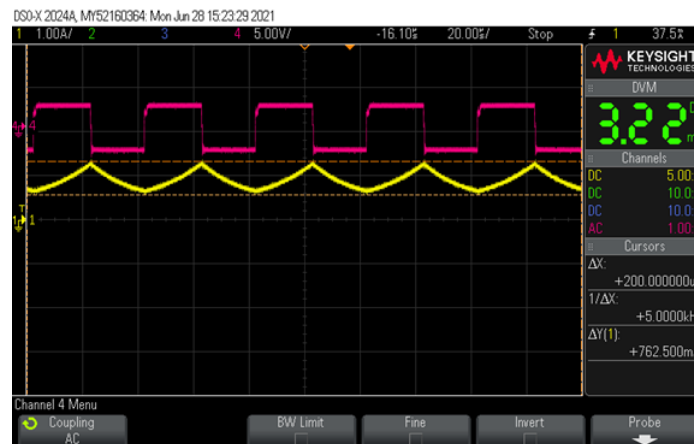


Figure 6.9: Biased inductor current waveform

6.3.1.1 Biased inductor Current Waveform analysis

When explaining the waveform figure 6.14 a slight slope is observed in the waveform. The observed waveform can be explained through figure 6.10. From the research paper [3] when the inductance vs current is mapped for the standard inductor and biased inductor there was an observation. When the current is at 0A the inductance of the standard inductor will be similar the case as for the designed inductance L , but for the biased inductor the inductance will be at reverse saturation point due to presence of the permanent magnet. Hence choosing magnet act as a crucial stage to not push the non linear region to bigger value. When observed in figure 6.14 and in simulation figure 6.5 the slope is visible at the starting point or initial point of charging of the inductor and move to the linear region. This doesn't affect the performance of the inductor until the maximum operation point lies below this non linear region.

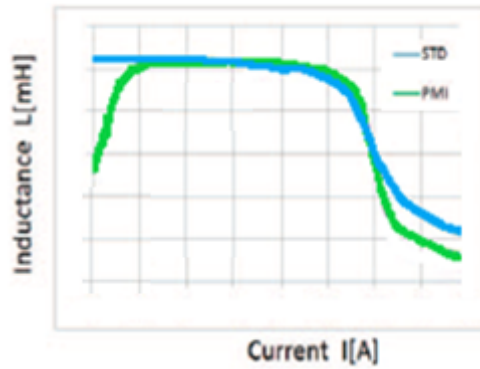


Figure 6.10: L vs I for standard and biased inductor

6.3.2 Diode Current Waveform

This section give the comparison of the diode current operation of both simulation and model output waveform



Figure 6.11: Diode current waveform

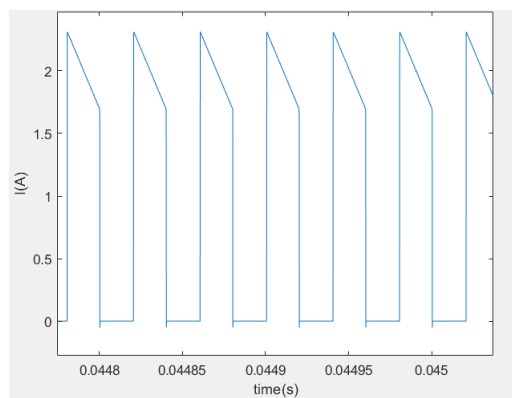


Figure 6.12: Diode current simulation waveform

6.3.3 Capacitor Current Waveform

This section give the comparison of the capacitor current operation of both simulation and model output waveform.

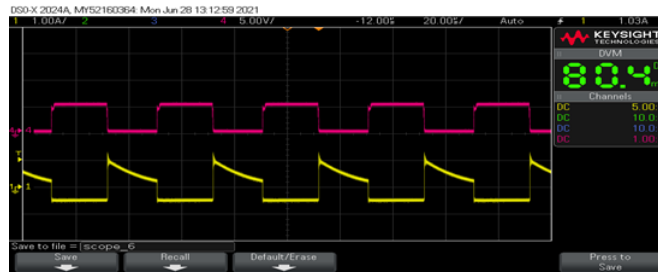


Figure 6.13: Capacitor Current Waveform

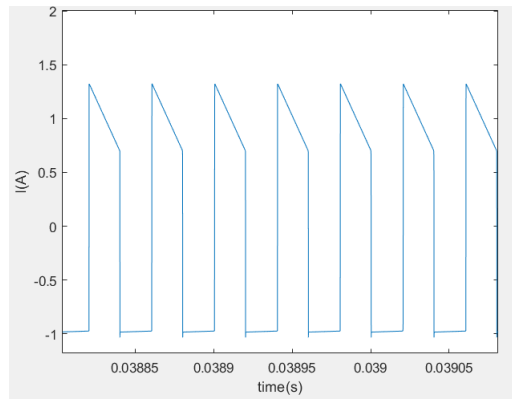


Figure 6.14: Capacitor current simulation waveform

7

Results and Discussion

In this section, the hardware testing results for both standard inductor- boost converter and biased inductor - boost converter are discussed. These results are compared and analyzed with the aim and scope of our thesis.

7.1 Standard and Biased Inductor - Boost converter test results

7.1.1 Power Comparison

The input of 12V is supplied to the boost converter through the regulated power supply and at the output we have used the 24 Ohms load as shown in figure 6.6 and figure 6.7. Due to some losses across the different components, the output voltage is not similar to what we expected. The gate pulse for the MOSFET is given by Arduino Nano at a frequency of 25kHz and 50% duty cycle. The power comparison of both the boost converter circuits are shown in table 7.1.

Table 7.1: Boost Converter Power Comparison

	Input Voltage (V)	Input Current (A)	Input power (W)	Output voltage (V)	Output Current (A)	Output Power (W)
Standard Inductor - Boost Converter	12	1.96	23.52	23	0.95	21.8
Biased Inductor - Boost converter	11.9	1.96	23.32	22.8	0.95	21.42

7.1.2 Loss Comparison

There are different losses we can find across the different component of a boost converter circuit which is shown in table 7.2. The aim of this test is to calculate losses across the core of an inductor. Since we are operating at very low power rating, it is difficult to calculate core losses practically. Hence, we theoretically calculated by subtracting the total power loss across the circuit and the losses measured across different components of the circuit.

Table 7.2: Different Losses across Boost Converter

	Standard Inductor - Boost Converter	Biased Inductor - Boost Converter
Conduction Losses of MOS-FET	29.5mW	29.34mW
Turn ON and Turn OFF Losses of MOSFET	40mW	39.6mW
Gate Charge or Input Capacitance Losses	3.93mW	3.93mW
Output Capacitance Loss	2.59mW	2.59mW
Diode Loss	1.10W	1.06W
Inductor Cu wire Loss	0.247W	0.104W
Total Loss (Excluding core losses)	1.42W	1.239W

Table 7.3: Core Loss of Standard and Biased Inductor

	Standard Inductor - Boost Converter	Biased Inductor - Boost Converter
Input Power	23.52W	23.32W
Output Power	21.8W	21.42W
Total Power Loss = I/p Power - O/p Power	1.72W	1.9W
Total Losses	1.42W	1.239W
Core Loss = Total Power loss - Total Loss	0.3W	0.66W

From table 7.3 we can observe that, the core losses across a biased inductor is high compared to a standard inductor. Since, in the biased inductor the core size is reduced by 4 times, as a result the flux density across the core material increases and hence the core saturates. The copper wire losses in the biased inductor is less compared to the standard inductor. Because, the number of turns in biased inductor is reduced by 2 times compared to the standard inductor.

There are possible ways to improve the analysis by considering the performance of the biased inductor both in high power mode and low power mode giving better judgement for the design and the performance of the biased inductor in the converter. Including a permanent magnet raise the issue of EMC, studying the effect of PM on the surrounding component will give a better judgement of the compatibility to use the biased inductor for designing the converter.

8

Conclusion

In this thesis, a biased inductor and a standard inductor is designed, simulated, and implemented in the boost converter operated at 25kHz frequency and verified using experimental testing. First, the design requirement is analysed creating a boost converter in LT-spice and taking the input needed for designing the inductor. A standard inductor with N27 material with $B_{sat}=0.5T$ and number of turns to be 42 as well as core sizing to be 25*20*13mm is simulated in COMSOL and FEMM. Designing of the biased inductor is considered keeping the standard inductor and then performing adjustments. The biased inductor has a permanent magnet introduced in order to increase the energy storage capacity of the inductor. The Choice of the permanent magnet with remanence(Br) to be 0.35T and as area of the permanent magnet of 470mm².

The designed biased inductor has an area of the cross-section that is smaller 4 times and the copper volume is reduced to 50% compared to the standard inductor. One of the main purposes for the design of a biased inductor is to study the weight improvement and it was observed that the weight of the biased inductor was reduced by 35% compared to the standard inductor. When both the inductor is implemented in the boost converter the efficiency was approximately the same 93%. However, the core loss of the biased inductor is increased by twice compared to the standard inductor which is as expected. Thus the efficiency remained the same with improvements in weight and performance for the biased inductor when its compared to the standard inductor.

8.1 Future Work

There are possible ways to improve the analysis by considering the performance of the biased inductor both in high power mode and low power mode giving better judgement for the design and the performance of the biased inductor in the converter.

Permanent magnet in inductor might raise the issue of EMC, studying the effect of PM on the surrounding component will give a better judgement of the compatibility to use the biased inductor when designing the converter.

8.2 Sustainable Aspects

The sustainable aspects of this thesis are explained in this section. The sustainability aspects of a boost converter using a standard and biased inductor materials and other components in the circuit is investigated. Its impact on the environment is studied. The core material used for the design of the inductor and the semiconductor components used for the circuit are considered for the environmental impacts in this thesis.

In the aerospace industry, the weight of the components used for various applications plays an important role to reduce the overall cost and environmental impact. In this type of industry, electrical components helps to reduce the cost, release of carbon dioxide to the environment and noise pollution. In order to achieve this goal, magnetically biased inductors helps to reduce the overall weight of the circuit and it reduces the core material (N27) and copper wire used for the production of the inductor. The selection of the core material and use of the rare earth magnets in this design helps the electrical circuit to operate more economically and efficiently.

The decrease in inductor weight using the biased inductor, reduces the overall weight of a boost converter circuit and the efficiency is almost equal when using a converter with a standard inductor. This decrease in weight and dimension reduces the size of a PCB board and number of components used for the design of a board. The overall reduction in the circuit helps to reduce the plastic and copper material used for the PCB design.

8.3 Ethical Aspects

Based on the IEEE code of ethics [21], the magnetically biased inductor in the switching converters are compared considering ethical aspects. We considered three IEEE code of ethical aspects in our thesis, which were illustrated in this section.

The first code of ethics is "to seek, accept, and offer honest criticism of technical work, to acknowledge and correct errors, to be honest, and realistic in stating claims or estimates based on available data, and to credit properly the contributions of others". In the magnetically biased inductor in the switching converters project, proper research has been conducted by comparing the converter circuit using both a standard and a biased inductor. Since the design is new and not fully exploited, it is important to present the data obtained during the design, simulation and testing of the converter, so that it would be helpful to analyze the effect of the magnets on the different components of the circuit or for the future projects.

The second code of ethics is "To improve the understanding of technology, its appropriate applications and potential consequences". In this thesis, the designing of the biased inductor and understanding of various test conditions were the major

important aspects which also helped when implementing the converter circuit.

The third code of ethics is "to avoid injuring others, their property, reputation, or employment by false or malicious actions". In order to follow this aspect, while designing the magnetically biased inductor, the proper calculations and the tests have been done.

8. Conclusion

Bibliography

- [1] Design, Analysis and Simulation of Magnetic Biased Inductors with Saturation-Gap Aguilar, Andres Revilla; Munk-Nielsen, Stig
- [2] N. Mohan, T. Underland, and W. Robbins, Power electronics converters, applications and design, 1. John Wiley and Sons INC, 1997, vol. 28, pp. 105–106.
- [3] Half Size Reduction of DC Output Filter Inductors With the Saturation-Gap Magnetic Bias Topology Andrés Revilla Aguilar, Member, IEEE, and Stig Munk-Nielsen, Member, IEEE
- [4] Comparison of Single-Layer and Multi-Layer Windings with Physical Constraints or Strong Harmonics M. E. Dale C. R. Sullivan
- [5] Method for introducing bias magnetization in ungaped cores: “The Saturation-Gap” Andrés Revilla Aguilar and Stig Munk-Nielsen Energy Technology dept. Aalborg University Aalborg, Denmark
- [6] Size Reduction of a DC Link Choke Using Saturation Gap and Biasing with Permanent Magnets, Aguilar, Andres Revilla; Munk-Nielsen, Stig; Zuccherato, Marco; Thougard, Hans-Jørgen, PCIM Europe 2014. International Exhibition and Conference for Power Electronics, Intelligent Motion, Renewable Energy and Energy Management Nuremberg, 20 – 22 May 2014, Proceedings.
- [7] Non-Isolated Dual Half-Bridge ZVS/ZCS High Step-Down Converter with Zero DC Bias Current Coupled Inductor and Active Clamp: K. I. Hwu, W. Z. Jiang, 2016 IEEE International Conference on Sustainable Energy Technologies (ICSET)
- [8] Energy Stored in Permanent Magnets, Howard C. Lovatt and Peter A. Watterson, IEEE TRANSACTIONS ON MAGNETICS, VOL. 35, NO. 1, JANUARY 1999
- [9] Design of Optimum Inductors Using Magnetically Hard Ferrites in Combination with Magnetically Soft Materials, J. T. Ludwig, J. Appl. Phys. 29, 497 (1958); doi: 10.1063/1.1723197

- [10] Inductors Biased with Permanent Magnets, J. T. LUDWIG, ASSOCIATE MEMBER AIEE, Digest of papers 60-198 and 60-199, recommended by the AIEE
- [11] Permanent Magnet Inductor Design, G. M. Shane and S. D. Sudhoff, 978-1-4244-9273-2/11/26.00 ©2011 IEEE
- [12] Design and Optimization of Permanent Magnet Inductors, G. M. Shane and S. D. Sudhoff, 978-1-4577-1216-6/12/26.00 ©2012 IEEE
- [13] Nonlinear inductors for active power factor correction circuits, A. Stadler, C. Gulden, T. Stolzke, 978-1-4673-1972-0/12/31.00 ©2012 IEEE
- [14] Design of a High-Temperature Pre-Biased Line Choke for Power Electronics Applications, Rafal Wrobel, Neville McNeill, and Phil H. Mellor, 978-1-4244-1668-4/08/25.00 ©2008 IEEE
- [15] Experimental Investigation of DC-Bias Related Core Losses in a Boost Inductor, Hiroyuki Kosai, Zafer Turgut, and James Scofield, IEEE TRANSACTIONS ON MAGNETICS, VOL. 49, NO. 7, JULY 2013
- [16] Influence of DC Bias on the Electrical Characteristics of SMD Inductors, Cedo J. Žlebić¹, Dragan R. Kljajić¹, Nelu V. Blaž¹, Ljiljana D. Živanov¹, Aleksandar B. Menićanin², and Mirjana S. Damnjanović¹, IEEE TRANSACTIONS ON MAGNETICS, VOL. 51, NO. 1, JANUARY 2015
- [17] Analysis and Modelling of a Permanent Magnet Biased Inductor Used in Motor Drive Systems, Marco Zuccherato, Firuz Zare, Chalmers University of Technology Sweden, IEEE Xplore
- [18] Design and Performance Analysis of Active Inductor with Low Voltage and High Q factor, R.C.Gurjar, Dr.D.K.Mishra, IEEE Xplore Part Number:CFP20F70-ART; ISBN:978-1-7281-4685-0
- [19] Erickson, Robert W. (Author). Fundamentals of Power Electronics. Second Edition. Secaucus, NJ, USA: Kluwer Academic Publishers, 2000.
- [20] Fundamentals of Power electronics with MATLAB, Ranadall Shaffer, second Edition, ISBN:1-58450-852-3
- [21] <https://www.ieee.org/content/dam/ieee-org/ieee/web/org/about/corporate/ieee-code-of-ethics.pdf>

A

Appendix 1

A.1 Aurdino Nano Code used in Boost Converter

```
include <PWM.h>
include <Arduino.h>
int potentiometer = A0; //Input from potentiometer
int feedback = A1; // Feedback input
int PWM = 3; // Digital pin for PWM signal
int pwm = 0; // Initial value of pwm width
int32_t frequency=25000;

void setup() {
  pinMode(potentiometer, INPUT);
  pinMode(feedback, INPUT);
  pinMode(PWM, OUTPUT);
}

void loop() {
  float voltage = analogRead(potentiometer); //We read the value of the
  potentiometer, which is the desired value
  // float output = analogRead(feedback); //We read the feedback, which is the real
  value
  //pwm = pwm+1;

  pwm = constrain(pwm, 10, 250);
  delay(1000);

  analogWrite(PWM, pwm); //Finally, we create the PWM signal
}
```